Electronic Profiling of *N*-Phosphine Oxide-Substituted Imidazolin-2-ylidenes (PoxIms) and Imidazolidin-2-ylidenes (SPoxIms)

Jia Nuo Leung,[a] Yutaka Mondori,[b] Sensuke Ogoshi,[b] Yoichi Hoshimoto,*[,b,c] and Han Vinh Huynh*[,a]

[a] Department of Chemistry, Faculty of Science, National University of Singapore, 3 Science Drive 3, Singapore 117453, Republic of Singapore

[b] Department of Applied Chemistry, Faculty of Engineering, Osaka University, Suita, Osaka 565-0871, Japan

[c] Center for Future Innovation (CFi), Division of Applied Chemistry, Faculty of Engineering, Osaka University, Suita, Osaka 565-0871, Japan

ABSTRACT: A detailed electronic study of the *N*-phosphine oxide functionalized imidazolin-2-ylidenes (PoxIms) and imidazolidin-2-ylidenes (SPoxIms) has been performed experimentally using IR, ^{13}C and ^{77}Se NMR spectroscopies. While the net donor/acceptor properties of the (S)PoxIms could not be differentiated via IR spectroscopy (TEP), NMR spectroscopic methods (HEP, Se) reveal that the (S)PoxIms are slightly weaker σ-donors, but stronger π-acceptors compared to common NHCs. Moreover, backbone and substituent-effects could also be resolved by the latter allowing for a ranking of their electronic properties. Finally, the donicities of these well-designed NHC ligands in their bidentate κ^2-C,O modes were evaluated using HEP2 and compared to those of classical chelators.

INTRODUCTION

Donor-functionalized N-heterocyclic carbenes (NHCs) have garnered much attention due to the possibility for hemilabile chelation or bimetallic complexation.[1–4] In particular, hemilability of the additional functional group allows for a strategic modulation of the ligand's overall electronic and steric properties. By careful design of the Lewis acid and interactions involved, these multifunctional NHCs can be applied for different purposes beyond their typical use as multidentate ligands.

Among the different classes of functionalized NHCs, the *N*-phosphine oxide-substituted imidazolin-2-ylidenes (PoxIms) and imidazolidin-2-ylidenes (SPoxIms) have demonstrated characteristic reactivity by exhibiting an assortment of monodentate, bidentate, or bridging coordination modes (Chart 1). Introduced by the group of Hoshimoto in 2015,[5] (S)PoxIm (includes both unsaturated PoxIm and saturated SPoxIm) ligands have been used in areas such as H_2 activation via frustrated Lewis pair (FLP) chemistry,[5] syntheses of mixed anhydrides,[6] programmable intramolecular transmetalation,[7] reversible chemisorption of carbon monoxide,[8] and Lewis acid-mediated modulation of a local environment surrounding a metal center.[9]

Due to the contrast between the soft character of the carbene donor and the hard nature of the phosphine oxide donor, the selective complexation on the carbene and/or oxygen atom(s) can be designed by judicious choice and stoichiometry of the Lewis acids (or Lewis acidic metals) added. In addition, different conformations of the bulky *tert*-butyl (^{t}Bu) units and smaller oxide unit on the phosphinoyl substituent allow for significant variation in the stereoelectronic properties of the ligand upon rotation of the N–P bond (Scheme 1).

Chart 1. (S)PoxIm ligands and their selected complexation modes.

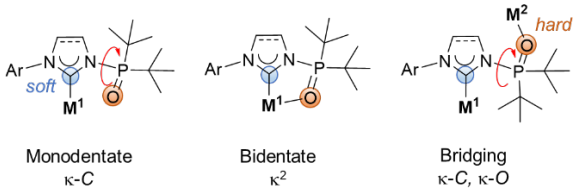

Generally, the *anti* orientation of the P=O bond to the carbene site is favored in the free (S)PoxIms because repulsion between the lone pairs of the two units should be minimized.[5] Upon monodentate coordination to a metal center by the carbene, steric repulsion between the (S)PoxIm and co-ligands can induce a rotation of the *N*-phosphinoyl group to the less sterically demanding *syn* conformer.[5,8,10,11] Thus far, retention of the *anti* conformer in κ-*C* (S)PoxIm monometallic complexes has only been observed for linear copper(I) and gold(I)[7,11] complexes with smaller co-ligands due to their higher spatial capacity to accommodate the bulkier ^{t}Bu groups.

While the steric requirements of (S)PoxIms have been quantified by the %V_{bur} methodology,[12] their electronic properties have not been comprehensively investigated and compared systematically. Herein, we present a σ-donor/π-acceptor evaluation of (S)PoxIms using three spectroscopic techniques, namely IR spectroscopy (Tolman electronic parameter, TEP),[13] ^{13}C NMR spectroscopy (Huynh electronic parameter, HEP),[14,15] and ^{77}Se NMR spectroscopy (Chart 2).[16]

Scheme 1. Generation of (S)PoxIms 2a–2e and scope in this study.

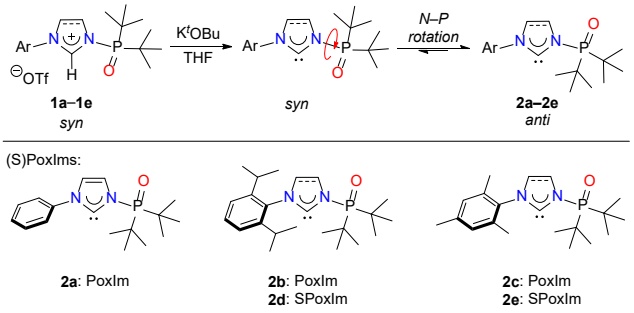

Importantly, the three electronic parameters measure different electronic aspects of ligands. Compared to the TEP which measures net σ-donor/π-acceptor abilities, the HEP primarily evaluates the σ-donor strengths of ligands. On the other hand, the ^{77}Se NMR chemical shifts of selenium NHC adducts allow for an understanding of the respective NHC's π-acceptor properties. A comparison of any trends in electronic properties between the monodentate and bidentate modes of coordination is also discussed.

Chart 2. Spectroscopic methods used for the electronic evaluation of (S)PoxIms.

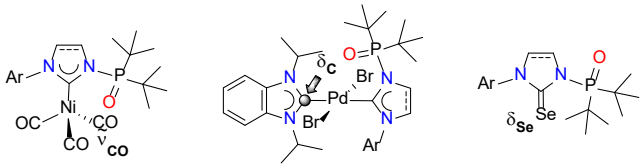

RESULTS AND DISCUSSION

Electronic evaluation of (S)PoxIms using A_1 CO stretching frequencies in nickel(0) complexes. Preparation of the (S)PoxIm precursor salts **1a–1e** and their respective (S)PoxIm carbenes **2a–2e** was carried out following reported procedures.[5,6] While the nickel(0) complexes **3b–3d** and **4b–4d** are known,[8] the new complex probes bearing the monodentate κ-*C* (S)PoxIms (**3a** and **3e**) and bidentate κ^2-(S)PoxIms (**4a** and **4e**) were obtained following an analogous approach (Scheme 2). The carbene center and phosphinoyl oxygen in the nickel(0) complexes exhibit a *syn* orientation, implying a rotation of the *N*-phosphinoyl bond to minimize the steric congestion around the tetrahedral metal center.

Using the [Ni(CO)$_3$L] complex probes **3a–3e** of the monodentate κ-*C* (S)PoxIm ligands, the A_1 CO stretching frequencies (TEP values) were obtained via IR spectroscopy. The TEP values of the κ-*C* (S)PoxIm ligands **2a**–**2e** are listed in Table 1 together with the literature TEP values[17] of 1,3-*bis*(2,6-diisopropylphenyl)imidazolin-2-ylidene (IPr), 1,3-*bis*(2,6-diisopropylphenyl)imidazolidin-2-ylidene (SIPr), 1,3-dimesitylimidazolin-2-ylidene (IMes), 1,3-dimesitylimidazolidin-2-ylidene (SIMes).

Scheme 2. Selective preparation of monodentate κ-*C* and bidentate κ^2-(S)PoxIm nickel(0) carbonyl complexes.

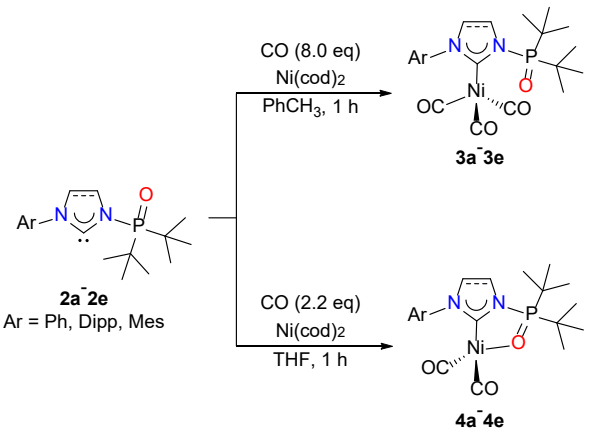

Table 1. TEP values of monodentate κ-*C* (S)PoxIm ligands measured in CH_2Cl_2.

(S)PoxIm	Complex	TEP [cm^{-1}]
κ-*C* **2a**	**3a**	2049
κ-*C* **2b**	**3b**	2048[a]
κ-*C* **2c**	**3c**	2048[a]
κ-*C* **2d**	**3d**	2049[a]
κ-*C* **2e**	**3e**	2049
IPr	[NiCO$_3$(IPr)]	2052[b]
IMes	[NiCO$_3$(IMes)]	2051[b]
SIPr	[NiCO$_3$(SIPr)]	2052[b]
SIMes	[NiCO$_3$(SIMes)]	2052[b]

[a] Taken from ref 8. [b] Taken from ref 17.

Overall, the TEP values obtained from **3a**–**3e** lie within a very limited range of only 1 cm^{-1} between 2048 to 2049 cm^{-1}. By assumption of a very optimistic standard deviation (σ) of 0.5 cm^{-1} for the A_1 bands, the net donor strengths of the κ-*C* (S)PoxIm ligands **2a**–**2e** cannot be differentiated by the carbonyl-based methodology within 3σ (>99%).[18] The inability of TEP to discern both the differences in *N*-aryl substituents and backbone (un)saturation makes it unsuitable for the detailed electronic evaluation of κ-*C* (S)PoxIms.

In comparison to the common NHCs (IMes/SIMes, IPr/SIPr) they appear to be marginally better net donors despite having an electron-withdrawing P^{V}O^{t}Bu$_2$ N-substituent (σ_m = 0.31, σ_p = 0.41), which is counter-intuitive.[19]

Table 2. The A_1 CO stretching frequencies of bidentate κ^2-(S)PoxIms nickel(0) complexes in CH_2Cl_2.

(S)PoxIm	Complex	A_1 band [cm^{-1}]
κ^2-**2a**	**4a**	2042
κ^2-**2b**	**4b**	2047[a]
κ^2-**2c**	**4c**	2046[a]
κ^2-**2d**	**4d**	2047[a]
κ^2-**2e**	**4e**	2042

[a] Taken from ref 8.

In contrast to the κ-*C*-coordinated (S)PoxIm complexes **3a**–**3e**, the A_1 CO stretching frequencies of the κ²-coordinated (S)PoxIm complexes **4a**–**4e** are generally lower {2042 to 2047 cm^{-1}, Table 2}. Due to the reduced number of carbonyl ligands in **4a**–**4e**, the π back-donation from the nickel(0) center to each carbonyl ligand is expectedly greater, leading to a further weakening of the remaining CO bonds and a decrease in wavenumber. While the same A_1 CO wavenumbers for the *N*-diisopropylphenyl (Dipp) substituted unsaturated κ²-**2b** and saturated κ²-**2d** were obtained, a significant difference in A_1 band was observed between the analogous *N*-mesityl (Mes) substituted κ²-**2c** (2046 cm^{-1}) and κ²-**2e** (2042 cm^{-1}). The A_1 CO stretching frequencies of 2046–2047 cm^{-1} for κ²-**2b**–**2d** are similar and higher than those for κ²-**2a** and κ²-**2e** (2042 cm^{-1}). Overall, there appears to be no clear trend in the CO stretching frequencies found in the κ²-(S)PoxIm complexes **4a**–**4e**, which suggests that the carbonyl-based methodology is unsuitable for the complete differentiation of bidentate (S)PoxIm ligands.

Synthesis of palladium(II) complexes bearing monodentate κ-*C* (S)PoxIm ligands. The preparation of the κ-*C* (S)PoxIm palladium(II) complex probes for HEP evaluation follows two methods (Scheme 3). Using the imidazolium salts **1a**–**1c**, a one-pot procedure involving a silver carbene transmetalation route (Method A) was performed with silver oxide, tetrabutylammonium bromide (TBAB), and the dipalladium precursor[20] $[PdBr_2(^iPr_2\text{-bimy})]_2$ (**I**) ($^iPr_2$-bimy = 1,3-diisopropylbenzimidazolin-2-ylidene). TBAB acts as a bromide source in this case for AgBr precipitation, which is a driving force for the silver carbene transmetalation. The unsaturated κ-*C* PoxIm palladium(II) complexes **5a**–**5c** were thus obtained in 79–91% yields after removal of the tetrabutylammonium salts via silica gel filtration. However, the same method could not be applied to the imidazolinium salts **1d** and **1e** due to their higher susceptibility to base-assisted hydrolytic ring opening side reactions.[21–23] To eliminate any traces of water in the reaction, the SPoxIm carbene ligands **2d** and **2e** were generated using potassium *tert*-butoxide under inert conditions before bridge cleavage of the $[PdBr_2(^iPr_2\text{-bimy})]_2$ (**I**) precursor (Method B), which afforded the κ-*C* SPoxIm palladium(II) complexes **5d** and **5e** in 65–68% yields.

Scheme 3. Preparation of κ-*C* (S)PoxIm HEP complex probes.

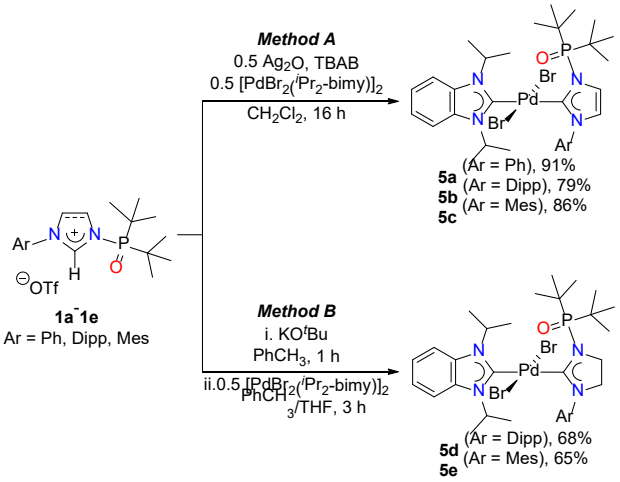

All palladium(II) complexes **5a**–**5e** are stable to air/moisture and have excellent solubilities in common organic solvents such as dichloromethane, chloroform, acetone, and ethyl acetate, and moderate solubilities in diethyl ether. Their formation was supported by positive mode ESI mass spectrometry, which shows base peaks for the $[M - Br]^+$ cations owing to the dissociation of one bromido ligand from the neutral complexes. In addition, their ^1H NMR spectra show an absence of the resonances for C2–H in **1a**–**1e**. The ^1H NMR signals for the isopropyl groups of the $^iPr_2$-bimy ligand appear as two septets and two doublets, which point towards hindered rotation about the Pd–C bonds. Strikingly, the two septets for the isopropyl CH protons are found at distinctly different chemical shift ranges of 5.16–5.54 ppm and 6.82–7.09 ppm. While the former is similar to those of analogous 1,3-diarylimidazolin-2-ylidene palladium(II) complexes,[14,24] the latter is significantly more downfield due to C–H···O interactions with the phosphine oxide moiety of the (S)PoxIm carbene (*vide infra*). Formation of *bis*-carbene complexes **5a**–**5e** was also confirmed by $^{13}C\{^1H\}$ NMR spectroscopy with the detection of the (S)PoxIm carbene doublets ($^2J_{C,P}$ = 11–13 Hz) between 184.5–214.4 ppm and $^iPr_2$-bimy carbene singlets between 176.9 to 178.24 ppm. The $^{31}P\{^1H\}$ NMR chemical shifts of the phosphinoyl group in **5a**–**5e** (58–62 ppm) are upfield shifted relative to the precursors **1a**–**1e** (70–78 ppm), reflecting an increased shielding on the phosphorous atom.

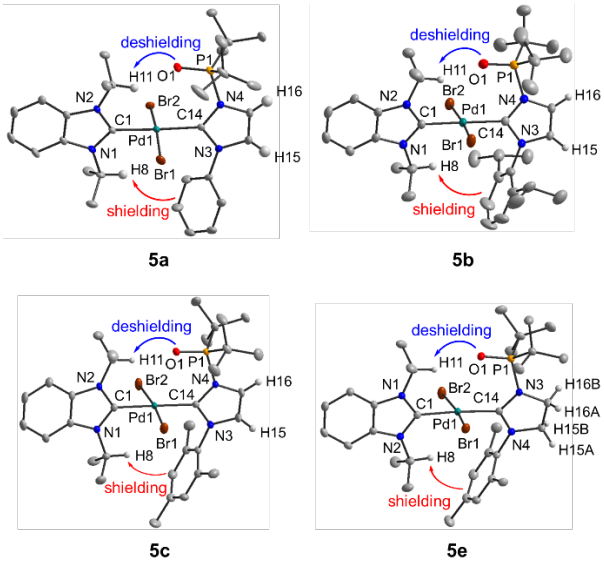

Figure 1. Solid-state molecular structures of **5a–5c** and **5e** showing 50% probability ellipsoids. Hydrogen atoms (except isopropyl C–H and (S)PoxIm backbone protons) and solvent molecules are omitted for clarity. Selected bond lengths [Å] and angles [°]: **5a**, Pd1–C1 2.003(4), Pd1–C14 2.022(4), Pd1–Br1 2.4525(6), Pd1–Br2 2.4410(7); C1–Pd1–C14 177.8(2), Br1–Pd1–Br2 171.23(2). **5b**, Pd1–C1 2.000(3), Pd1–C14 2.039(2), Pd1–Br1 2.4364(7), Pd1–Br2 2.4508(7); C1–Pd1–C14 178.8(1), Br1–Pd1–Br2 174.31(2). **5c**, Pd1–C1 1.997(1), Pd1–C14 2.049(1), Pd1–Br1 2.4497(5), Pd1–Br2 2.4555(5); C1–Pd1–C14 178.79(6), Br1–Pd1–Br2 173.02(2). **5e**, Pd1–C1 1.987(2), Pd1–C14 2.042(2), Pd1–Br1 2.4578(5), Pd1–Br2 2.4576(4); C1–Pd1–C14 176.15(7), Br1–Pd1–Br2 170.88(2).

The solid-state molecular structures of **5a**–**5c** and **5e** obtained by single crystal X-ray diffraction analyses are depicted in Figure 1. The palladium(II) centers show essentially square planar geometries with calculated τ_4 values close to 0 (perfect square planar geometry)[25] between 0.05 (**5b**) to 0.09 (**5e**). The two carbenes are coordinated in an almost perpendicular manner between 78–

90° to the [$PdBr_2C_2$] coordination plane *trans* to each other. Notably, these complexes feature solely monodentate κ-*C* coordination of the (S)PoxIm carbene ligands **2a**–**2e**, which is rare considering that only bidentate κ^2-*C,O* or mixed monodentate κ-*C* /bidentate κ^2-*C,O* (S)PoxIm coordination to Pd^{II} centers are known thus far.[10,26]

While the bulkier mesityl and diisopropylphenyl substituents in **5b**, **5c**, and **5e** adopt almost perpendicular configurations to the NHC plane (dihedral angles θ = 81–87°), the less sterically encumbered phenyl substituent in **5a** is twisted at a smaller θ of 55° from the carbene plane. The bond parameters around the palladium center in the three complexes are similar to those of previously reported[14] HEP complexes bearing classical NHCs, and the isopropyl CH protons are oriented towards the metal center indicative of C–H···Pd anagostic interactions.[20,27] In addition, one of the isopropyl CH protons (H11) is located in relatively close proximities of 2.19–2.44 Å to the phosphinoyl oxygen, which suggests the presence of additional C–H···O interactions. The significant downfield shift of the isopropyl CH proton in the ^{1}H NMR spectra points towards a retention of such interactions in solution as well. Notably, the C–H···O interactions feature angles of 146 to 164°, although it remains uncertain whether these interactions can be classified as weak hydrogen bonds or merely electrostatic attractions.[28–31]

σ-Donor strength evaluation of monodentate κ-*C* (S)PoxIm ligands by HEP. For determination of ligand donor strength by the Huynh electronic parameter, the ^{i}Pr$_2$-bimy $^{13}C_{carbene}$ NMR shifts in **5a**–**5e**, also known as HEP values, are obtained and listed in Table 3. A more downfield shift or larger HEP value indicates a stronger σ-donating *trans* co-ligand, whereas a more upfield shift or smaller HEP value is induced by a weaker σ-donor. An assessment of the HEP values for the κ-*C* (S)PoxIm ligands shows that they are expectedly weaker than other classical *N*-alkyl substituted NHCs and within the range of *N*-aryl substituted NHCs such as IPr and IMes.[32]

Table 3. HEP values of monodentate κ-*C* (S)PoxIm ligands measured in $CDCl_3$. [a]

(S)PoxIm	Complex	HEP [ppm]
κ-*C* **2a**	**5a**	178.2_4
κ-*C* **2b**	**5b**	177.3_2
κ-*C* **2c**	**5c**	176.8_9
κ-*C* **2d**	**5d**	177.6_7
κ-*C* **2e**	**5e**	177.1_6
IPr	-	177.5_2 [b]
IMes	-	177.2_2 [b]
SIPr	-	177.6_3 [b]
SIMes	-	177.5_9 [b]
SIPrPh	-	178.7_0 [c]

[a] Referenced to 77.7 ppm with second decimal place in subscript, given an estimated standard deviation of 0.01 ppm.[32] [b] Taken from ref 14. [c] Taken from ref 24.

With the exception of SIPr, the replacement of an aryl substituent in IPr and (S)IMes with a di-^{t}butylphosphine oxide group leads to a decrease in donating ability due to its stronger electron-withdrawing effect (σ_m = 0.31, σ_p = 0.41).[19] Presumably, the combined negative inductive effect of the diisopropylphenyl and phosphinoyl substituents in κ-*C* **2d** is counteracted by the electron-releasing character of the saturated backbone, resulting in a similar donicity to SIPr. In addition, the larger HEP values of κ-*C* **2d** (177.6_7 ppm) and κ-*C* **2e** (177.1_6 ppm) compared to their respective unsaturated analogues κ-*C* **2b** (177.3_2 ppm) and κ-*C* **2c** (176.8_9 ppm) indicate that the saturated SPoxIms are stronger donors than their unsaturated PoxIm counterparts. This result is also consistent with the trend observed in previously reported classical NHCs (e.g. SIPr > IPr; SIMes > IMes, Table 3, Figure 2).[14]

A ranking of the κ-*C* (S)PoxIm σ-donor strengths can be established from their HEP values in the order κ-*C* **2c** < **2e** < **2b** < **2d** < **2a** (Figure 2). By closer inspection of the unsaturated PoxIms κ-*C* **2a**–**2c,** the σ-donicity increases in the aryl substituent order mesityl (Mes, 176.8_9 ppm) < diisopropylphenyl (Dipp, 177.3_2 ppm) < phenyl (Ph, 178.2_4 ppm). The same trend has been observed in classical imidazolin-2-ylidenes[24] {IMes < IPr < SIPr < SIPrPh, (Figure 2)} and ammonium-functionalized 1,2,4-triazolin-5-ylidenes.[33] The higher donicity of the Ph substituent can be explained by its higher flexibility to rotate around the N–C bond, which enhances its positive mesomeric (+*M*) effect.[33–36] In comparison, the sterically bulky Mes and Dipp substituents are preferentially oriented perpendicular to the carbene plane (*vide supra*), which diminishes their +*M* contributions, leading to lower donicities of their NHCs. This phenomenon has also been previously discussed in detail by experimental and computational methods.[33,37] Overall, the HEP values of κ-*C* **2a**–**2e** can be found in the range 176.9–178.3 ppm spanning ~1.4 ppm. Given an average standard deviation σ of 0.01 ppm in the ^{i}Pr$_2$-bimy carbene NMR signal,[32] even the small differences in aryl substituents and backbone saturation of the (S)PoxIm ligands can be unambiguously detected by the Huynh electronic parameter.

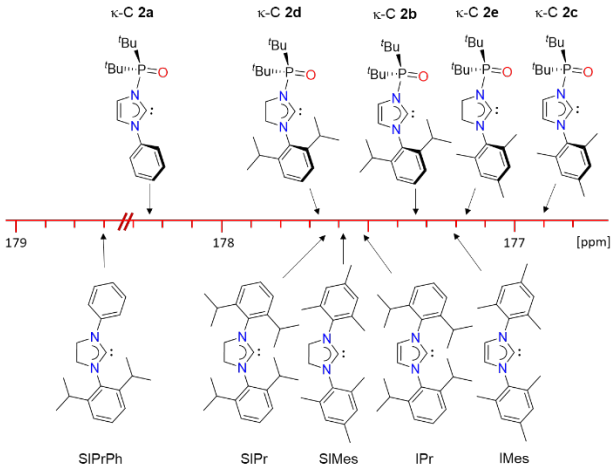

Figure 2. σ-donor strength comparison of monodentate κ-*C* (S)PoxIms on the ^{13}C NMR scale.

Synthesis of palladium(II) complexes bearing bidentate κ^2-(S)PoxIm ligands. The HEP concept has also been extended for the donor strength assessment of popular bidentate ligands (HEP2) such as dicarbenes,[38] neutral/monoanionic diimines,[38–41] dithiocarbamates,[42] β-ketiminates,[43] and monoanionic C^N chelators.[44] Hence, we sought to evaluate the donor strength abilities of the charge-neutral bidentate κ^2-(S)PoxIm ligands using HEP2 complex probes of the type [PdBr(^{i}Pr$_2$-bimy)(L^1^L^2)]PF_6 {L^1^L^2 = charge-neutral and unsymmetrical chelator for evaluation}.

The required HEP2 complexes bearing bidentate κ^2-(S)PoxIm ligands could be prepared by the abstraction of a bromido ligand

from their HEP complexes **5a**–**5e** with concurrent chelate formation via coordination of the phosphinoyl oxygen atoms (Scheme 4). Due to the formation of some side products during an initial reaction with silver hexafluorophosphate at ambient temperature, the bromido abstraction reactions were subsequently carried out at 0 °C for a shorter period of time. By strict control of stoichiometry and temperature, the cationic complexes **6a**–**6e** could be obtained in excellent yields of >85% as yellow powders (Scheme 4). Generally, they are well-soluble in common polar organic solvents such as chloroform and acetone. However, they exhibit lower solubilities than their neutral precursors **5a**–**5e** in non-polar organic solvents, and are not soluble in diethyl ether.

Scheme 4. Synthesis of bidentate κ²-(S)PoxIm HEP2 complexes.

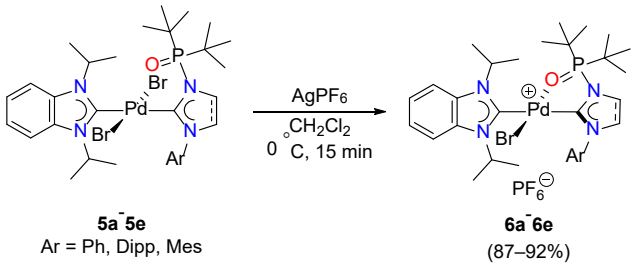

5a–**5e**
Ar = Ph, Dipp, Mes

6a–**6e**
(87–92%)

Upon coordination of the phosphinoyl oxygen to the palladium center, an essentially coplanar orientation of the (S)PoxIm ligand to the [PdBrC$_2$O] coordination plane is enforced, which eliminates any C–H···O interactions between the isopropyl C–H moiety of ^{i}Pr$_2$-bimy and phosphinoyl oxygen. Accordingly, the isopropyl C–H protons of **6a**–**6e** are detected as a single septet between 5.92–6.03 ppm in their ^{1}H NMR spectra compared to two septets in the HEP complexes **5a**–**5e**. Furthermore, downfield shifts of 0.49–0.76 and 0.25–0.37 ppm for the isopropyl C–H and CH$_3$ NMR signals are detected due to a minimization of the shielding effect from the aryl substituents which are almost perpendicular to the isopropyl groups in **6a**–**6e** (Figures 1 and 3).

Chelation of the κ²-(S)PoxIm ligand in **6a**–**6e** was also confirmed by the identification of the ^{i}Pr$_2$-bimy ^{13}C$_{carbene}$ NMR signals between 168.8–170.9 ppm with small ^3J(C,P) coupling constants of 4 Hz and (S)PoxIm ^{13}C$_{carbene}$ NMR signals between 176.7–201.3 ppm ($^2J_{C,P}$ = 15 Hz). The carbene chemical shifts in **6a**–**6e** are lower than those in complexes **5a**–**5e** (*vide supra*), which is indicative of a more Lewis acidic palladium center and in line with the formation of cationic complexes. Coordination of the phosphinoyl oxygen atom to the palladium(II) center also pulls electron density away from the phosphorous atom, leading to more downfield ^{31}P NMR signals between 98–102 ppm compared to 58–62 ppm in complexes **5a**–**5e** bearing monodentate κ-*C* (S)PoxIm ligands. While positive mode ESI mass spectrometry shows the same *m/z* base peaks as **5a**–**5e** for the [M – PF$_6$]$^+$ cation, *m/z* base peaks for the PF$_6^-$ anion are also identified in the negative mode ESI mass spectra of **6a**–**6e**.

The solid-state molecular structures of **6b** and **6d** (Figure 3) indeed confirm an essentially coplanar arrangement of the bidentate PoxIm ligand to the [PdBrC$_2$O] coordination plane {RMSD of [C1Pd1O1P1N4C14Br1] plane = 0.056 Å (**6b**) and 0.045 Å (**6d**)} with an average bite angle of 84°. Both structures have a calculated τ$_4$ index of 0.06, which indicates retention of a square planar geometry (*vide supra*). On the other hand, the ^{i}Pr$_2$-bimy carbene maintains a perpendicular orientation to the square plane, hence breaking the isopropyl C–H···O interaction noted for complexes **5a**–**5e**. Moreover, the aryl substituent on the bidentate (S)PoxIm ligand is now positioned next to the bromido ligand and away from the ^{i}Pr$_2$-bimy carbene, leading to an absence of the shielding effect on the ^{i}Pr$_2$-bimy isopropyl group (*vide supra*). Generally, both Pd–C bonds are slightly longer than those in the neutral complex structures **5a**–**5c** and **5e**. The P=O bond distance between 1.510(3)–1.513(3) Å is also elongated from those in **5a**–**5c** and **5e** between 1.470(3)–1.475(1) Å due to the donation of electron density from the oxygen atom to the palladium(II) center. In addition, the diisopropylphenyl substituents in **6b** and **6d** are oriented at almost perpendicular angles of θ = 87–88° from the carbene plane, and a slight increase of θ from 81° in the monodentate κ-C (S)PoxIm complex **5b** to 87° in the bidentate κ²-(S)PoxIm complex **6b** is observed to minimize steric congestion with the adjacent bromido ligand.

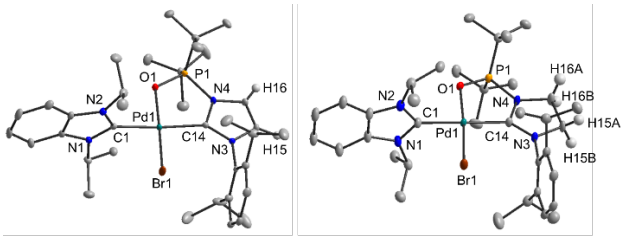

6b **6d**

Figure 3. Solid-state molecular structures of **6b** and **6d** showing 30% probability ellipsoids. Hydrogen atoms (except (S)PoxIm backbone protons), PF$_6^-$ anions, and disorder of the molecule in **6d** are omitted for clarity. Selected bond lengths [Å] and angles [°]: **6b**, Pd1–C1 2.018(4), Pd1–C14 2.068(4), Pd1–O1 2.083(3), Pd1–Br1 2.3809(6), P1–O1 1.510(3); C1–Pd1–C14 175.9(2), Br1–Pd1–O1 176.08(9), O1–Pd1–C14 83.5(1). **6d**, Pd1–C1 2.010(3), Pd1–C14 2.049(3), Pd1–O1 2.078(2), Pd1–Br1 2.392(1), P1–O1 1.513(3); C1–Pd1–C14 174.5(1), Br1–Pd1–O1 176.36(9), O1–Pd1–C14 83.7(1).

Donor strength evaluation of bidentate κ²-(S)PoxIm ligands by HEP2. The HEP2 values of the bidentate κ²-(S)PoxIm ligands obtained from the ^{i}Pr$_2$-bimy ^{13}C$_{carbene}$ NMR chemical shifts in complexes **6a**–**6e** are listed in Table 4. Owing to the *cis*-coordination of the ^{i}Pr$_2$-bimy ligand to the phosphinoyl moiety, three-bond coupling between the carbene and phosphorous atom is detected, and the coupling constants are also shown in Table 4.

Strikingly, the trend in HEP2 values of the unsaturated PoxIms κ²-**2a**–**2c** for the aryl substituents (Figure 4) is exactly reverse to that of the monodentate PoxIms, where κ²-**2a** (Ph, 168.7$_7$ ppm) < κ²-**2b** (Dipp, 169.4$_3$ ppm) < κ²-**2c** (Mes, 169.9$_5$ ppm). It should be noted that the steric bulk of the (S)PoxIm ligand around the metal center is enhanced upon bidentate κ²-coordination and ensuing coplanar orientation in all complexes **6a**–**6e**. Moreover, the adjacent position of the bromido ligand to the (S)PoxIm aryl substituent hinders the rotation around the N–C$_{aryl}$ away from the preferred perpendicular orientation to the carbene plane. Consequently, the +*M* effect of the aryl substituents is expected to be minimal, and their negative inductive effect (−*I*) becomes dominant. By consideration of the chiefly inductive effects, Ph is expected to be more electron-withdrawing than the Mes and Dipp substituents, leading to the lowest HEP2 value. While it is hard to differentiate the small electronic effects between Mes and Dipp, the spatial occupancy (%V_{bur}) of Dipp around the metal center is higher than that of Mes because of the bulkier isopropyl groups.[24] The steric encumbrance of the Dipp substituent in κ²-

2b within the more congested environment of bidentate complexes **6a**–**6e** can thus push the bromido ligand closer to the $^{i}Pr_2$-bimy carbene, leading to an upfield shift in the HEP2 value from an increased shielding effect of the lone pairs on the bromido ligand.

Table 4. HEP2 values of bidentate κ²-(S)PoxIm ligands measured in $CDCl_3$. [a]

(S)PoxIm	Complex	HEP2 [ppm]	$^{3}J_{C,P}$ [Hz]
κ²-**2a**	**6a**	168.7_7	3.5
κ²-**2b**	**6b**	169.4_3	3.7
κ²-**2c**	**6c**	169.9_5	3.6
κ²-**2d**	**6d**	170.1_3	4.0
κ²-**2e**	**6e**	170.8_8	3.5

[a] Referenced to 77.7 ppm with second decimal place in subscript, given an estimated standard deviation of 0.01 ppm.[32].

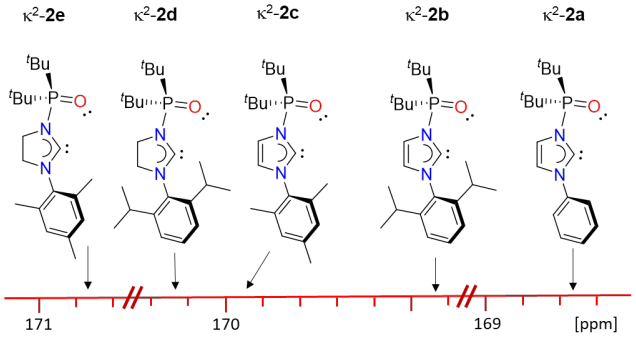

Figure 4. Donor strength comparison of bidentate κ²-(S)PoxIms on the HEP2 scale.

Similar to the monodentate κ-*C* (S)PoxIm ligands, the donating abilities of the saturated κ²-**2d** (170.1_3 ppm) and κ²-**2e** (170.8_8 ppm) are stronger than their respective unsaturated analogues κ²-**2b** (169.4_3 ppm) and κ²-**2c** (169.9_5 ppm) (Figure 4). The difference is more pronounced (ΔHEP2 = 0.7–0.9 ppm) compared to in the monodentate ligands (ΔHEP = 0.3–0.4 ppm) presumably due to the electronic distribution across two donor sites in a bidentate coordination mode. Overall, the bidentate κ²-(S)PoxIm ligands are weaker donors than diNHCs (177–180 ppm),[38] dithiocarbamates/xanthates (174–179 ppm),[42] and monoanionic C^N chelators (176–185 ppm),[43,44] but stronger donors than neutral diimines (157–164 ppm).[15,40] Their donicities are similar to that of N^O β-ketiminate chelators (NacAcs) (~170 ppm)[43] and lie in the higher donor range of monoanionic N^N chelators (165–173 ppm).[40,41]

Selenium adducts of (S)PoxIms. Using the ^{77}Se NMR chemical shifts of NHC-selenium adducts, the relative π-acidities of the respective NHCs can be estimated. The methodology was introduced by Ganter in 2013,[16] where increased backdonation from selenium to the NHC would lead to deshielding and thus downfield shifts in the ^{77}Se NMR signal of the selenium-adducts. Accordingly, the selenium-NHC adducts **7a–7e** of the (S)PoxIms were prepared by stirring elemental selenium with the free NHCs **2a–2e** in THF (Scheme 5).[8] Molecular structures of **7b–7d** from a previous study[8] and **7a** and **7e** (Supporting Information) show a retention of the *anti* conformation between the carbene center and the P=O unit in the selenium adducts, which is likely due to the low steric constraints by the single selenium atom and repulsion between the lone pairs on the selenium and oxygen atoms.

Scheme 5. Preparation of (S)PoxIm selenium adducts.

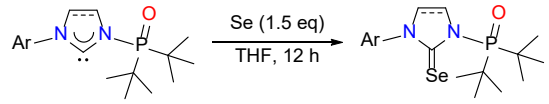

2a–**2e**
Ar = Ph, Dipp, Mes

7a–**7e**

The ^{77}Se NMR signals of the selenium-(S)PoxIm adducts **7a**–**7e** measured in acetone-d_6 are shown in Figure 5 together with those of the classical NHCs (IPr, IMes, SIPr, SIMes).[16,45,46] Substitution of one aryl group in the respective classical NHCs with a phosphinoyl moiety leads to a marked increase in π-acidity as evident from the large downfield shifts of ~84–114 ppm in ^{77}Se NMR signals. In addition, the π-acidity influenced by different aryl substituents increases in the order Mes (**2c**, 149 ppm) < Ph (**2a**, 163 ppm) < Dipp (**2b**, 178 ppm). Saturation of the backbone also increases the amount of backdonation {**2b** (178 ppm) < **2d** (265 ppm); **2c** (149 ppm) < **2e** (216 ppm)} in a similar trend to the classical NHCs (Figure 5).

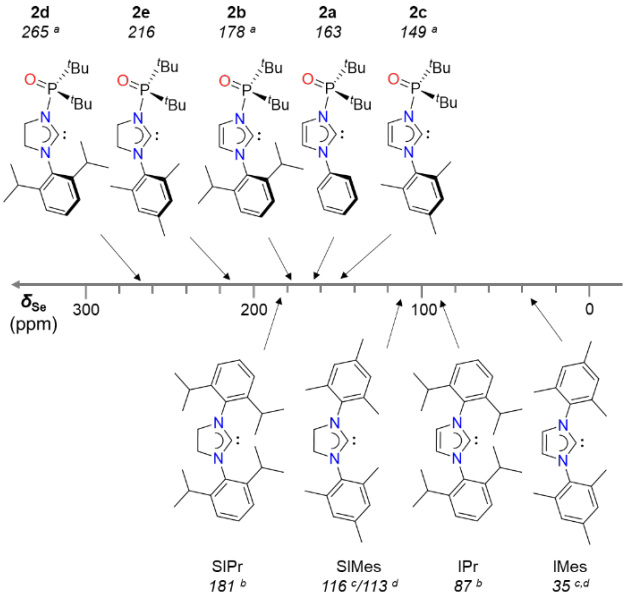

Figure 5. π-acceptor properties of (S)PoxIms on the ^{77}Se NMR scale (measured in acetone-d_6). [a] Taken from ref 8. [b] Taken from ref 16. [c] Taken from ref 45. [d] Taken from ref 46.

CONCLUSION

A series of nickel(0), palladium(II), and selenium compounds were prepared for the detailed electronic evaluation of the (S)PoxIm NHCs using the Tolman electronic parameter (TEP), Huynh electronic parameter (HEP), and ^{77}Se NMR spectroscopy. While the TEP was unable to distinguish the net σ-donor/π-acceptor properties of the *syn* configured κ-C (S)PoxIm ligands, the HEP indicate that they are slightly weaker σ-donors compared to their classical NHC analogues. Notably, ^{77}Se NMR spectroscopic measurements reveal that *anti* configured (S)PoxIm ligands are stronger π-acceptors than their classical NHC analogues, which

agrees with the introduction of an electron-withdrawing P^V group. Moreover, assessment of the bidentate κ^2-(S)PoxIm ligands via HEP2 puts their donor strengths between that of diNHCs and monoanionic N^N chelators. The ability of the (S)PoxIm ligands to coordinate in different modes resulting in different electronic properties warrants further studies of their applications in various areas.

EXPERIMENTAL SECTION

General Considerations. Unless otherwise noted, all manipulations were conducted under an inert atmosphere using standard Schlenk line or dry box techniques. New compounds are characterized by a combination of ^{1}H, ^{13}C{^{1}H}, ^{31}P{^{1}H}, ^{19}F{^{1}H}, and ^{77}Se{^{1}H} NMR spectroscopy, LRMS, HRMS (ESI/EI), IR spectroscopy and elemental analysis. ^{1}H and ^{13}C{^{1}H} NMR spectra were recorded at 298 K on a Bruker DRX 400 (400 MHz) or Bruker AVANCE I 500 (500 MHz) spectrometers, and the chemical shifts (δ) were internally referenced to the residual solvent signals relative to tetramethylsilane (^{1}H,^{13}C). The chemical shifts in the ^{31}P{^{1}H} and ^{19}F{^{1}H} NMR spectra were recorded relative to H_3PO_4 and $CFCl_3$ respectively. The chemical shifts in the ^{77}Se{^{1}H} NMR spectra were recorded relative to KSeCN as an external standard. All ^{13}C{^{1}H} spectra of HEP/HEP2 complexes measured in $CDCl_3$ are referenced at 77.70 ppm. ESI mass spectra were measured using a Finnigan MAT LCQ spectrometer. Elemental analyses were performed on a Thermo Flashsmart CHNS/O Elemental Analyzer. Precursor salts **1a**–**1e**,[5,6,9] (S)PoxIm carbenes **2a**–**2e**,[5,6,9] complexes **3b–3d**,[5,6] complex **4b–4e**,[5,6,9] and selenium adducts **7b**–**7d**,[8] and complex **I**[14] were synthesized following reported procedures. Experimental details for complexes **3a**, **3e**, **4a** and selenium adducts **7a** and **7e** are given in the Supporting Information. No uncommon hazards are noted.

General procedure for the preparation of palladium complexes 5a–5c. This reaction was carried out without exclusion of moisture or air under ambient conditions. A suspension of 1-di*t*butylphosphine oxide-3-arylimidazolium triflate **1a–1c** (0.17 mmol), silver oxide (0.09 mmol), tetrabutylammonium bromide (0.18 mmol), and complex **I** (0.09 mmol) in CH_2Cl_2 (20 mL) was stirred at ambient temperature for 16 h shielded from light. The resulting suspension was filtered over Celite and the solvent was removed under vacuum. A silica gel filtration was carried out using ethyl acetate or diethyl ether as the eluent. Removal of the volatiles *in vacuo* afforded the complexes as a yellow powder.

***trans*-dibromido(1,3-diisopropylbenzimidazolin-2-ylidene)(1-di*t*butylphosphine oxide-3-phenylimidazolin-2-ylidene)palladium(II) (5a).** Silica gel filtration was performed using ethyl acetate as the eluent. Crystals were obtained by layer diffusion of hexane into an ethyl acetate solution. Yield: 120 mg (0.16 mmol, 91%). ^{1}H NMR (500 MHz, $CDCl_3$): δ = 8.14 (m, 2 H, Ar–H), 7.58 (m, 2 H, Ar–H), 7.53 (m, 2 H, Ar–H), 7.42 (m, 1 H, Ar–H), 7.29 (m, 1 H, Ar–H), 7.24 (m, 1 H, Ar–H), 7.09 (m, 3 H, Ar–H and NC*H*$(CH_3)_2$), 5.54 (m, ^3J(H,H) = 7.1 Hz, 1 H, NC*H*$(CH_3)_2$), 1.69–1.68 (d, ^3J(H,H) = 7.1 Hz, 6 H, NCH(C*H*$_3)_2$), 1.49 (m, ^3J(H,P) = 15.1 Hz, 24 H, C$(CH_3)_3$ and NCH(C*H*$_3)_2$). ^{13}C{^{1}H} NMR (125.77 MHz, $CDCl_3$): δ = 184.4$_7$ (d, ^2J(C,P) = 11.9 Hz, PhPoxIm $C_{carbene}$), 178.2$_4$ (^{i}Pr$_2$-bimy $C_{carbene}$), 141.4, 134.5, 134.3, 129.3, 129.2, 129.1, 128.5, 128.3, 124.1 (d, J(C,P) = 3.4 Hz), 122.2 (d, J(C,P) = 4.7 Hz), 121.9, 121.8, 113.2, 112.9 (Ar–C), 54.0, 53.6 (N*C*H$(CH_3)_2$), 38.8 (d, ^1J(C,P) = 66.9 Hz, *C*$(CH_3)_3$), 28.2 (C(*C*H$_3)_3$), 21.4, 21.3 (NCH(*C*H$_3)_2$). ^{31}P{^{1}H} NMR (202 MHz, $CDCl_3$): δ = 62.0. Anal calcd. for $C_{30}H_{43}Br_2N_4OPPd$: C, 46.62; H, 5.61; N, 7.25. Found: C, 46.31; H, 5.42; N, 7.40. HRMS (ESI): calcd for $[M - Br]^+$, $C_{30}H_{43}BrN_4OPPd^+$, *m/z* 691.1392; found, *m/z* 691.1394 (100).

***trans*-dibromido(1,3-diisopropylbenzimidazolin-2-ylidene)(1-di*t*butylphosphine oxide-3-(2,6-diisopropylphenyl)imidazolin-2-ylidene)palladium(II) (5b).** Silica gel filtration was performed using diethyl ether as the eluent. Yield: 115 mg (0.13 mmol, 79%). ^{1}H NMR (500 MHz, $CDCl_3$): δ = 7.52 (m, 2 H, Ar–H), 7.38 (m, 2 H, Ar–H), 7.33 (m, 1 H, Ar–H), 7.29 (s, 1 H, Ar–H), 7.16 (m, 1 H, Ar–H), 7.04 (m, 2 H, Ar–H), 6.87 (m, ^3J(H,H) = 7.0 Hz, 1 H, NC*H*$(CH_3)_2$), 5.29 (m, ^3J(H,H) = 7.0 Hz, 1 H, NC*H*$(CH_3)_2$), 3.12 (m, ^3J(H,H) = 6.7 Hz, 2 H, Dipp C*H*$(CH_3)_2$), 1.70–1.68 (d, ^3J(H,H) = 7.0 Hz, 6 H, NCH(C*H*$_3)_2$), 1.52–1.49 (d, ^3J(H,P) = 15.0 Hz, 18 H, C$(CH_3)_3$), 1.39–1.37 (d, ^3J(H,H) = 6.7 Hz, 6 H, Dipp CH(C*H*$_3)_2$), 1.33–1.32 (d, ^3J(H,H) = 7.0 Hz, 6 H, NCH(C*H*$_3)_2$), 1.01–1.00 (d, ^3J(H,H) = 6.7 Hz, 6 H, Dipp CH(C*H*$_3)_2$). ^{13}C{^{1}H} NMR (125.77 MHz, $CDCl_3$): δ = 187.0$_5$ (d, ^2J(C,P) = 11.8 Hz, DippPoxIm $C_{carbene}$), 177.3$_2$ (^{i}Pr$_2$-bimy $C_{carbene}$), 147.9, 136.8, 134.4 (×2), 130.4, 126.7 (d, J(C,P) = 3.0 Hz), 124.2, 121.7, 121.6, 121.0 (d, J(C,P) = 4.9 Hz), 113.1, 112.7 (Ar–C), 53.7, 53.6 (N*C*H$(CH_3)_2$), 38.8 (d, ^1J(C,P) = 66.7 Hz, *C*$(CH_3)_3$), 29.5, 28.3 (C(*C*H$_3)_3$), 27.3, 23.6, 21.3 (NCH(*C*H$_3)_2$), 21.2 (NCH(*C*H$_3)_2$). ^{31}P{^{1}H} NMR (202 MHz, $CDCl_3$): δ = 61.2. Anal calcd. for $C_{36}H_{55}Br_2N_4OPPd$: C, 50.45; H, 6.47; N, 6.54. Found: C, 50.92; H, 6.49; N, 6.32. HRMS (ESI): calcd for $[M - Br]^+$, $C_{36}H_{55}BrN_4OPPd^+$, *m/z* 775.2333; found, *m/z* 775.2342 (100).

***trans*-dibromido(1,3-diisopropylbenzimidazolin-2-ylidene)(1-di*t*butylphosphine oxide-3-mesitylimidazolin-2-ylidene)palladium(II) (5c).** Silica gel filtration was performed using ethyl acetate as the eluent. Crystals were obtained by layer diffusion of hexane into a chloroform solution. Yield: 120 mg (0.15 mmol, 86%). ^{1}H NMR (500 MHz, $CDCl_3$): δ = 7.50 (m, 1 H, Ar–H), 7.36 (m, 1 H, Ar–H), 7.30 (m, 1 H, Ar–H), 7.07 (m, 5 H, Ar–H), 6.82 (m, ^3J(H,H) = 7.0 Hz, 1 H, NC*H*$(CH_3)_2$), 5.36 (m, ^3J(H,H) = 7.0 Hz, 1 H, NC*H*$(CH_3)_2$), 2.43 (s, 3 H, Mes *p*-CH_3), 2.32 (s, 6 H, Mes *o*-CH_3), 1.70–1.69 (d, ^3J(H,H) = 7.0 Hz, 6 H, NCH(C*H*$_3)_2$), 1.50–1.47 (d, ^3J(H,P) = 15.0 Hz, 18 H, C$(CH_3)_3$), 1.39–1.38 (d, ^3J(H,H) = 7.0 Hz, 6 H, NCH(C*H*$_3)_2$). ^{13}C{^{1}H} NMR (125.77 MHz, $CDCl_3$): δ = 186.1$_0$ (d, ^2J(C,P) = 11.4 Hz, MesPoxIm $C_{carbene}$), 176.8$_9$ (^{i}Pr$_2$-bimy $C_{carbene}$), 139.2, 137.5, 136.8, 134.4 (×2), 129.4, 124.5 (d, J(C,P) = 3.0 Hz), 122.4, 122.3, 121.7 (d, J(C,P) = 4.7 Hz), 113.2, 112.7 (Ar–C), 53.8, 53.7 (N*C*H$(CH_3)_2$), 38.7 (d, ^1J(C,P) = 66.8 Hz, *C*$(CH_3)_3$), 28.3 (C(*C*H$_3)_3$), 21.8 (Mes *p*-CH_3), 21.3, 21.1 (NCH(*C*H$_3)_2$), 20.7 (Mes *o*-CH_3). ^{31}P{^{1}H} NMR (202 MHz, $CDCl_3$): δ = 61.2. Anal calcd. for $C_{33}H_{49}Br_2N_4OPPd$: C, 48.63; H, 6.06; N, 6.87. Found: C, 48.44; H, 5.93; N, 6.80. HRMS (ESI): calcd for $[M - Br]^+$, $C_{33}H_{49}BrN_4OPPd^+$, *m/z* 733.1863; found, *m/z* 733.1864 (100).

General procedure for the preparation of palladium complexes 5d and **5e.** A solution of potassium *tert*-butoxide (1.3 eq) in toluene (5 mL) was added to a suspension of 1-di*t*butylphosphine oxide-3-arylimidazolinium triflate **1d** or **1e** (1 eq) in toluene (1 mL) and stirred for 1 h. The suspension was filtered into a solution of complex **I** (0.5 eq) in tetrahydrofuran (5 mL). The resulting solution was stirred for 3 h and the solvent was pumped away. The residue was washed with hexane to afford the compound as a yellow powder.

***trans*-dibromido(1,3-diisopropylbenzimidazolin-2-ylidene)(1-di*t*butylphosphine oxide-3-(2,6-diisopropyl-imidazolidin)-2-ylidene)palladium(II) (5d).** The reaction was carried out with 0.36 mmol of **1d**. Yield: 200 mg (0.23 mmol, 65%). ^{1}H NMR (500 MHz, $CDCl_3$): δ = 7.45 (m, 2 H, Ar–H), 7.33 (m, 3 H, Ar–H), 7.03 (m, 2 H, Ar–H), 6.96 (m, ^3J(H,H) = 7.0 Hz, 1 H, NC*H*$(CH_3)_2$), 5.16 (m, ^3J(H,H) = 7.0 Hz, 1 H, NC*H*$(CH_3)_2$), 4.02 (m, 4 H, Im–H), 3.52 (m, ^3J(H,H) = 6.7 Hz, 2 H, Dipp C*H*$(CH_3)_2$), 1.64–1.63 (d, ^3J(H,H) = 7.0 Hz, 6 H, NCH(C*H*$_3)_2$), 1.55–1.52 (d, ^3J(H,P) = 14.4 Hz, 18 H, C$(CH_3)_3$), 1.48–1.46 (d, ^3J(H,H) = 6.7 Hz, 6 H, Dipp CH(C*H*$_3)_2$), 1.29–1.28 (d, ^3J(H,H) = 7.0 Hz, 6 H, NCH(C*H*$_3)_2$), 1.13–1.12 (d, ^3J(H,H) = 6.7 Hz, 6 H, Dipp CH(C*H*$_3)_2$). ^{13}C{^{1}H} NMR (125.77 MHz, $CDCl_3$): δ = 212.5$_5$ (d, ^2J(C,P) = 13.1 Hz, DippSPoxIm $C_{carbene}$), 177.6$_7$ (^{i}Pr$_2$-bimy $C_{carbene}$), 148.7, 136.9, 134.5, 134.4, 130.4, 129.7, 124.5, 121.6 (×2), 113.1, 112.7 (Ar–C), 55.5, 53.6, 53.4, 49.9 (Im–C and N*C*H$(CH_3)_2$), 38.6 (d, ^1J(C,P) =

69.7 Hz, $C(CH_3)_3$), 29.6, 29.0 ($C(CH_3)_3$), 27.9, 24.4, 21.2 (×2) ($NCH(CH_3)_2$). $^{31}P\{^1H\}$ NMR (202 MHz, $CDCl_3$): δ = 57.6. Anal calcd. for $C_{36}H_{57}Br_2N_4OPPd$: C, 50.33;H, 6.69; N, 6.52. Found: C, 49.38; H, 6.37; N, 5.99. EAL results for the SPoxIm palladium complexes are generally unsatisfactory despite multiple attempts at purification and drying, possibly due to ring-opening/decomposition during combustion. HRMS (ESI): calcd for $[M - Br]^+$, $C_{36}H_{57}BrN_4OPPd^+$, *m/z* 777.2489; found, *m/z* 777.2500 (100).

***trans*-dibromido(1,3-diisopropylbenzimidazolin-2-ylidene)(1-di^{t}butylphosphine oxide-3-mesitylimidazolidi-n-2-ylidene)palladium(II) (5e).** The reaction was carried out with 0.21 mmol of **1e**. Crystals were obtained by layer diffusion of hexane into an ethyl acetate solution. Yield: 80 mg (0.10 mmol, 46%). ^1H NMR (500 MHz, $CDCl_3$): δ = 7.48 (m, 1 H, Ar–H), 7.34 (m, 1 H, Ar–H), 7.05 (m, 2 H, Ar–H), 7.03 (s, 2 H, Mes Ar–H), 6.89 (m, ^3J(H,H) = 7.0 Hz, 1 H, $NCH(CH_3)_2$), 5.21 (m, ^3J(H,H) = 7.0 Hz, 1 H, $NCH(CH_3)_2$), 4.06 (m, 2 H, Im–H), 3.90 (m, 2 H, Im–H), 2.54 (s, 6 H, Mes *o*-CH_3), 2.39 (s, 3 H, Mes *p*-CH_3), 1.65–1.63 (d, ^3J(H,H) = 7.0 Hz, 6 H, $NCH(CH_3)_2$), 1.53–1.50 (d, ^3J(H,P) = 14.4 Hz, 18 H, $C(CH_3)_3$), 1.35–1.33 (d, ^3J(H,H) = 7.0 Hz, 6 H, $NCH(CH_3)_2$). $^{13}C\{^1H\}$ NMR (125.77 MHz, $CDCl_3$): δ = 214.4$_4$ (d, ^2J(C,P) = 12.7 Hz, MesSPoxIm $C_{carbene}$), 177.1$_6$ (^{i}Pr$_2$-bimy $C_{carbene}$), 138.6, 138.0, 136.6, 134.5, 134.3, 129.7, 121.7, 121.6, 113.2, 112.7 (Ar–C), 53.8, 53.5, 52.5, 50.1 (Im–C and $NCH(CH_3)_2$), 38.5 (d, ^1J(C,P) = 69.9 Hz, $C(CH_3)_3$), 28.9 ($C(CH_3)_3$), 21.8, 21.3, 21.1, 21.0 ($NCH(CH_3)_2$ and Mes CH_3). $^{31}P\{^1H\}$ NMR (202 MHz, $CDCl_3$): δ = 57.7. Anal calcd. for $C_{33}H_{51}Br_2N_4OPPd$: C, 48.51; H, 6.29; N, 6.86. Found: C, 46.50; H, 5.69; N, 6.73. EAL results for the SPoxIm palladium complexes are generally unsatisfactory despite multiple attempts at purification and drying, possibly due to ring-opening/decomposition during combustion. HRMS (ESI): calcd for $[M - Br]^+$, $C_{33}H_{51}BrN_4OPPd^+$, *m/z* 735.2019; found, *m/z* 735.2022 (100).

General procedure for the preparation of palladium complexes 6a–6e. This reaction was carried out without exclusion of moisture or air under ambient conditions. Silver hexafluorophosphate (1 eq) was added to a solution of complex **5a–5e** (1 eq) in CH_2Cl_2 (5 mL) at 0 °C. The resulting suspension was stirred for 15 min and the solids were removed by filtration. The solvent was removed *in vacuo* and the residue was washed with hexane (3 × 2 mL) and dried, affording the product as a yellow powder.

Bromido(1,3-diisopropylbenzimidazolin-2-ylidene)(1-di^{t}butylphosphine oxide-3-phenylimidazolin-2-ylidene-κ^2-*C,O*)palladium(II) hexafluorophosphate (6a). The reaction was carried out with 0.08 mmol of **5a**. Yield: 60 mg (0.07 mmol, 92%). ^1H NMR (500 MHz, $CDCl_3$): δ = 7.78–7.77 (d, 1 H, Ar–H), 7.62–7.60 (dd, 2 H, Ar–H), 7.47 (m, 3 H, Ar–H), 7.43 (m, 3 H, Ar–H), 7.29–7.27 (dd, 2 H, Ar–H), 6.03 (m, ^3J(H,H) = 7.0 Hz, 1 H, $NCH(CH_3)_2$), 1.79–1.77 (d, ^3J(H,H) = 7.0 Hz, 6 H, $NCH(CH_3)_2$), 1.73–1.72 (d, ^3J(H,H) = 7.0 Hz, 6 H, $NCH(CH_3)_2$), 1.50–1.47 (d, ^3J(H,P) = 16.5 Hz, 18 H, $C(CH_3)_3$). $^{13}C\{^1H\}$ NMR (125.77 MHz, $CDCl_3$): δ = 176.6$_8$ (d, ^2J(C,P) = 15.0 Hz, PhPoxIm $C_{carbene}$), 168.7$_7$ (d, ^3J(C,P) = 3.5 Hz, ^{i}Pr$_2$-bimy $C_{carbene}$), 138.8, 133.8, 130.5, 129.8, 129.2 (d, *J*(C,P) = 4.1 Hz), 127.8, 123.7, 122.0 (d, *J*(C,P) = 5.1 Hz), 113.7 (Ar–C), 54.7 ($NCH(CH_3)_2$), 38.7 (d, ^1J(C,P) = 58.7 Hz, $C(CH_3)_3$), 26.4 ($C(CH_3)_3$), 22.3, 21.7 ($NCH(CH_3)_2$). $^{31}P\{^1H\}$ NMR (202 MHz, $CDCl_3$): δ = 102.21 (s, P=O), −142.32 (m, ^1J(P,F) = 712 Hz, PF_6). $^{19}F\{^1H\}$ NMR (471 MHz, $CDCl_3$): δ = −72.75 (d, ^1J(P,F) = 712 Hz, PF_6). Anal calcd. for $C_{30}H_{43}BrF_6N_4OP_2Pd$: C, 43.00; H, 5.17; N, 6.69. Found: C, 42.65; H, 5.34; N, 6.97. MS (ESI): calcd for $[M - PF_6]^+$, $C_{30}H_{43}BrN_4OPPd^+$, *m/z* 693; found, *m/z* 693 (100); calcd for $[M - PF_6 - Br - H]^+$, $C_{30}H_{42}N_4OPPd^+$, *m/z* 611; found, *m/z* 611 (50). HRMS (ESI): calcd for $[M - PF_6]^+$, $C_{30}H_{43}BrN_4OPPd^+$, *m/z* 691.1393; found, *m/z* 691.1395.

Bromido(1,3-diisopropylbenzimidazolin-2-ylidene)(1-di^{t}butylphosphine oxide-3-(2,6-diisopropylphenyl)imid-azolin-2-ylidene-κ^2-*C,O*)palladium(II) hexafluorophosphate (6b). The reaction was carried out with 0.07 mmol of **5b**. Yield: 58 mg (0.06 mmol, 90%). ^1H NMR (500 MHz, $CDCl_3$): δ = 7.90 (d, 2 H, Ar–H), 7.59–7.57 (dd, 2 H, Ar–H), 7.45 (t, ^3J(H,H) = 7.8 Hz, 1 H, Dipp Ar–H), 7.27 (m, 3 H, Ar–H), 7.22–7.21 (d, ^3J(H,H) = 7.8 Hz, 2 H, Dipp Ar–H), 5.97 (m, ^3J(H,H) = 7.1 Hz, 2 H, $NCH(CH_3)_2$), 2.44 (m, ^3J(H,H) = 6.9 Hz, 2 H, Dipp $CH(CH_3)_2$), 1.77–1.76 (d, ^3J(H,H) = 7.1 Hz, 6 H, $NCH(CH_3)_2$), 1.69–1.68 (d, ^3J(H,H) = 7.1 Hz, 6 H, $NCH(CH_3)_2$), 1.51–1.48 (d, ^3J(H,P) = 16.6 Hz, 18 H, $C(CH_3)_3$), 1.40–1.39 (d, ^3J(H,H) = 6.9 Hz, 6 H, Dipp $CH(CH_3)_2$), 1.17–1.16 (d, ^3J(H,H) = 6.9 Hz, 6 H, Dipp $CH(CH_3)_2$). $^{13}C\{^1H\}$ NMR (125.77 MHz, $CDCl_3$): δ = 178.8$_3$ (d, ^2J(C,P) = 14.9 Hz, DippPoxIm $C_{carbene}$), 169.4$_3$ (d, ^3J(C,P) = 3.7 Hz, ^{i}Pr$_2$-bimy $C_{carbene}$), 145.1, 135.3, 133.8, 131.3, 129.4 (d, *J*(C,P) = 3.5 Hz), 124.5, 123.7, 122.2 (d, *J*(C,P) = 4.7 Hz), 113.6 (Ar–C), 54.7 ($NCH(CH_3)_2$), 38.8 (d, ^1J(C,P) = 58.9 Hz, $C(CH_3)_3$), 29.7 (Dipp $CH(CH_3)_2$), 26.3 ($C(CH_3)_3$), 25.0, 23.9 (Dipp $CH(CH_3)_2$), 22.3, 21.5 ($NCH(CH_3)_2$). $^{31}P\{^1H\}$ NMR (202 MHz, $CDCl_3$): δ = 101.75 (P=O), −144.30 (m, ^1J(P,F) = 713 Hz, PF_6). $^{19}F\{^1H\}$ NMR (471 MHz, $CDCl_3$): δ = −72.58 (d, ^1J(P,F) = 713 Hz, PF_6). Anal calcd. for $C_{36}H_{55}BrF_6N_4OP_2Pd$: C, 46.89; H, 6.01; N, 6.08. Found: C, 46.41; H, 5.95; N, 5.63. MS (ESI): calcd for $[M - PF_6]^+$, $C_{36}H_{55}BrN_4OPPd^+$, *m/z* 777; found, *m/z* 777 (100); calcd for $[M - PF_6 - Br - H]^+$, $C_{36}H_{54}N_4OPPd^+$, *m/z* 695; found, *m/z* 695 (15). HRMS (ESI): calcd for $[M - PF_6]^+$, $C_{36}H_{55}BrN_4OPPd^+$, *m/z* 775.2333; found, *m/z* 775.2338.

Bromido(1,3-diisopropylbenzimidazolin-2-ylidene)(1-di^{t}butylphosphine oxide-3-mesitylimidazolin-2-ylidene-κ^2-*C,O*)palladium(II) hexafluorophosphate (6c). The reaction was carried out with 0.07 mmol of **5c**. Yield: 59 mg (0.07 mmol, 91%). ^1H NMR (500 MHz, $CDCl_3$): δ = 7.89–7.88 (d, 1 H, Ar–H), 7.61–7.59 (dd, 2 H, Ar–H), 7.29–7.28 (dd, 2 H, Ar–H), 7.17 (m, 1 H, Ar–H), 6.94 (s, 2 H, Ar–H), 5.98 (m, ^3J(H,H) = 7.0 Hz, 1 H, $NCH(CH_3)_2$), 2.32 (s, 3 H, Mes *p*-CH_3), 2.07 (s, 6 H, Mes *o*-CH_3), 1.79–1.77 (d, ^3J(H,H) = 7.0 Hz, 6 H, $NCH(CH_3)_2$), 1.74–1.73 (d, ^3J(H,H) = 7.0 Hz, 6 H, $NCH(CH_3)_2$), 1.50–1.47 (d, ^3J(H,P) = 16.5 Hz, 18 H, $C(CH_3)_3$). $^{13}C\{^1H\}$ NMR (125.77 MHz, $CDCl_3$): δ = 177.3$_5$ (d, ^2J(C,P) = 14.7 Hz, MesPoxIm $C_{carbene}$), 169.9$_5$ (d, ^3J(C,P) = 3.6 Hz, ^{i}Pr$_2$-bimy $C_{carbene}$), 140.4, 135.5, 134.7, 133.8, 129.7, 128.4 (d, *J*(C,P) = 4.0 Hz), 123.7, 122.7 (d, *J*(C,P) = 4.9 Hz), 113.6 (Ar–C), 54.7 ($NCH(CH_3)_2$), 38.7 (d, ^1J(C,P) = 59.0 Hz, $C(CH_3)_3$), 26.3 ($C(CH_3)_3$), 22.4 ($NCH(CH_3)_2$), 21.9 (Mes *p*-CH_3), 21.7 ($NCH(CH_3)_2$), 18.5 (Mes *o*-CH_3). $^{31}P\{^1H\}$ NMR (202 MHz, $CDCl_3$): δ = 101.69 (P=O), −144.33 (m, ^1J(P,F) = 712 Hz, PF_6). $^{19}F\{^1H\}$ NMR (471 MHz, $CDCl_3$): δ = −72.88 (d, ^1J(P,F) = 712 Hz, PF_6). Anal calcd. for $C_{33}H_{49}BrF_6N_4OP_2Pd$: C, 45.04; H, 5.61; N, 6.37. Found: C, 44.98; H, 5.45; N, 6.30. HRMS (ESI): calcd for $[M - PF_6]^+$, $C_{33}H_{49}BrN_4OPPd^+$, *m/z* 733.1863; found, *m/z* 733.1864 (100).

Bromido(1,3-diisopropylbenzimidazolin-2-ylidene)(1-di^{t}butylphosphine oxide-3-(2,6-diisopropylphenyl)imidazolidin-2-ylidene-κ^2-*C,O*)palladium(II) hexafluorophosphate (6d). The reaction was carried out with 0.09 mmol of **5d**. Yield: 78 mg (0.08 mmol, 91%). ^1H NMR (500 MHz, $CDCl_3$): δ = 7.57–7.55 (dd, 2 H, Ar–H), 7.36 (t, ^3J(H,H) = 7.8 Hz, 1 H, Dipp Ar–H), 7.26 (m, 3 H, Ar–H), 7.17–7.16 (d, ^3J(H,H) = 7.8 Hz, 2 H, Dipp Ar–H), 5.92 (m, ^3J(H,H) = 7.0 Hz, 2 H, $NCH(CH_3)_2$), 4.32 (t, ^3J(H,H) = 9.9 Hz, 2 H, Im–H), 4.18 (t, ^3J(H,H) = 9.9 Hz, 2 H, Im–H), 2.89 (m, ^3J(H,H) = 6.8 Hz, 2 H, Dipp $CH(CH_3)_2$), 1.74–1.73 (d, ^3J(H,H) = 7.0 Hz, 6 H, $NCH(CH_3)_2$), 1.65–1.64 (d, ^3J(H,H) = 7.0 Hz, 6 H, $NCH(CH_3)_2$), 1.49 (m, ^3J(H,P) = 15.8 Hz, 24 H, $C(CH_3)_3$ and Dipp $CH(CH_3)_2$), 1.31–1.30 (d, ^3J(H,H) = 6.8 Hz, 6 H, Dipp $CH(CH_3)_2$). $^{13}C\{^1H\}$ NMR (125.77 MHz, $CDCl_3$): δ = 201.3$_0$ (d, ^2J(C,P) = 16.1 Hz, DippSPoxIm $C_{carbene}$), 170.1$_3$ (d, ^3J(C,P) = 4.0 Hz, ^{i}Pr$_2$-bimy $C_{carbene}$), 145.2, 135.3, 133.7, 130.6, 124.9, 123.6, 113.6 (Ar–C), 58.6 (d, ^2J(C,P) = 2.9 Hz, Im–C), 54.7 ($NCH(CH_3)_2$), 48.4 (Im–C), 38.7 (d, ^1J(C,P) = 62.7 Hz, $C(CH_3)_3$), 29.7 (Dipp $CH(CH_3)_2$), 26.9 ($C(CH_3)_3$), 25.4, 24.5 (Dipp $CH(CH_3)_2$), 22.2, 21.3 ($NCH(CH_3)_2$).

$^{31}P\{^{1}H\}$ NMR (202 MHz, $CDCl_3$): δ = 98.07 (P=O), −144.36 (m, ^{1}J(P,F) = 712 Hz, PF_6). $^{19}F\{^{1}H\}$ NMR (471 MHz, $CDCl_3$): δ = −73.16 (d, ^{1}J(P,F) = 712 Hz, PF_6). Anal calcd. for $C_{36}H_{57}BrF_6N_4OP_2Pd$: C, 46.79; H, 6.22; N, 6.06. Found: C, 45.31; H, 5.79; N, 5.84. EAL results for the SPoxIm palladium complexes are generally unsatisfactory despite multiple attempts at purification and drying, possibly due to ring-opening/decomposition during combustion. HRMS (ESI): calcd for $[M - PF_6]^+$, $C_{36}H_{57}BrN_4OPPd^+$, *m/z* 777.2490; found, *m/z* 777.2509 (100).

Bromido(1,3-diisopropylbenzimidazolin-2-ylidene)(1-di^{t}butylphosphine oxide-3-mesitylimidazolidin-2-ylidene -κ^2-*C,O*)palladium(II) hexafluorophosphate (6e). The reaction was carried out with 0.10 mmol of **5e**. Yield: 75 mg (0.09 mmol, 87%). ^{1}H NMR (500 MHz, $CDCl_3$): δ = 7.59 (m, 3 H, Ar–H), 7.28–7.27 (dd, 2 H, Ar–H), 6.88 (s, 2 H, Mes Ar–H), 5.92 (m, ^{3}J(H,H) = 7.0 Hz, 2 H, NC*H*$(CH_3)_2$), 4.27 (m, 2 H, Im–H), 4.11 (m, 2 H, Im–H), 2.30 (s, 6 H, Mes *o*-CH_3), 2.27 (s, 3 H, Mes *p*-CH_3), 1.77–1.75 (d, ^{3}J(H,H) = 7.0 Hz, 6 H, NCH(C*H*$_3)_2$), 1.72–1.70 (d, ^{3}J(H,H) = 7.0 Hz, 6 H, NCH(C*H*$_3)_2$), 1.51–1.48 (d, ^{3}J(H,P) = 15.8 Hz, 18 H, $C(CH_3)_3$). $^{13}C\{^{1}H\}$ NMR (125.77 MHz, $CDCl_3$): δ = 200.1$_5$ (d, ^{2}J(C,P) = 16.2 Hz, MesSPoxIm $C_{carbene}$), 170.8$_8$ (d, ^{3}J(C,P) = 3.6 Hz, $^{i}Pr_2$-bimy $C_{carbene}$), 139.6, 135.6, 134.8, 133.8, 130.0, 123.6, 113.6 (Ar–C), 56.4 (d, ^{2}J(C,P) = 2.9 Hz, Im–C), 54.7 (N*C*H$(CH_3)_2$), 48.1 (Im–C), 38.7 (d, ^{1}J(C,P) = 62.8 Hz, *C*$(CH_3)_3$), 27.0 (C(*C*$H_3)_3$), 22.3, 21.8, 21.7, 18.6 (NCH(*C*$H_3)_2$ and Mes CH_3). $^{31}P\{^{1}H\}$ NMR (202 MHz, $CDCl_3$): δ = 98.17 (P=O), −144.32 (m, ^{1}J(P,F) = 713 Hz, PF_6). $^{19}F\{^{1}H\}$ NMR (471 MHz, $CDCl_3$): δ = −72.82 (m, ^{1}J(P,F) = 713 Hz, PF_6). Anal calcd. for $C_{33}H_{51}BrF_6N_4OP_2Pd$: C, 44.94; H, 5.83; N, 6.35. Found: C, 43.41; H, 5.55; N, 6.05. EAL results for the SPoxIm palladium complexes are generally unsatisfactory despite multiple attempts at purification and drying, possibly due to ring-opening/decomposition during combustion. MS (ESI): calcd for $[M - PF_6]^+$, $C_{33}H_{51}BrN_4OPPd^+$, *m/z* 737; found, *m/z* 737 (100); calcd for $[M - PF_6 - Br - H]^+$, $C_{33}H_{50}N_4OPPd^+$, *m/z* 655; found, *m/z* 655 (10). HRMS (ESI): calcd for $[M - PF_6]^+$, $C_{33}H_{51}BrN_4OPPd^+$, *m/z* 735.2020; found, *m/z* 735.2029.

ASSOCIATED CONTENT

Syntheses, characterization, and molecular structures of compounds **3a**, **3e**, **4a**, **7a**, and **7e**, correlation plots, NMR, IR, and ESI/EI-MS spectra, and selected crystallographic data (PDF).

This material is available free of charge via the Internet at http://pubs.acs.org.

Accession Codes

CCDC 2143034, 2143036, 2143044, 2321579–2321584, and 2321922–2321923 contain the supplementary crystallographic data for this paper. These data can be obtained free of charge via www.ccdc.cam.ac.uk/data_request/cif, or by emailing data_request@ccdc.cam.ac.uk, or by contacting The Cambridge Crystallographic Data Centre, 12 Union Road, Cambridge CB2 1EZ, UK; fax: +44 1223 336033.

AUTHOR INFORMATION

Corresponding Author

Han Vinh Huynh − *Department of Chemistry, Faculty of Science, National University of Singapore, Singapore 117543*; orcid.org/0000-0003-4460-6066; Email: chmhhv@nus.edu.sg

Yoichi Hoshimoto − *Department of Applied Chemistry, Faculty of Engineering, Osaka University, Suita, Osaka 565-0871, Japan*; *Center for Future Innovation (CFi), Division of Applied Chemistry, Faculty of Engineering, Osaka University, Suita, Osaka 565-0871, Japan*; orcid.org/0000-0003-0882-6109; Email: hoshimoto@chem.eng.osaka-u.ac.jp

Author

Jia Nuo Leung − *Department of Chemistry, Faculty of Science, National University of Singapore, Singapore 117543;* orcid.org/0000-0002-2240-3068

Yutaka Mondori − *Department of Applied Chemistry, Faculty of Engineering, Osaka University, Suita, Osaka 565-0871, Japan*

Sensuke Ogoshi − *Department of Applied Chemistry, Faculty of Engineering, Osaka University, Suita, Osaka 565-0871, Japan;* orcid.org/0000-0003-4188-8555

Notes

The authors declare no competing financial interest.

ACKNOWLEDGMENT

The authors thank the Singapore Ministry of Education and the National University of Singapore for financial support (WBS R-143-000-669-112). A part of this work was supported by Grants-in-Aid for Scientific Research (C) (21K05070), and Grants-in-Aid for Transformative Research Area (A) Digitalization-driven Transformative Organic Synthesis (22H05363). Technical support from staff at the Chemical, Molecular and Materials Analysis Centre (CMMAC) of the Chemistry Department at the National University of Singapore is appreciated.

REFERENCES

(1) Normand, A. T.; Cavell, K. J. Donor-Functionalised N-Heterocyclic Carbene Complexes of Group 9 and 10 Metals in Catalysis: Trends and Directions. *Eur. J. Inorg. Chem.* **2008**, 2781–2800.

(2) Hameury, S.; De Frémont, P.; Braunstein, P. Metal Complexes with Oxygen-Functionalized NHC Ligands: Synthesis and Applications. *Chem. Soc. Rev.* **2017**, *46*, 632–733.

(3) Evans, K. J.; Mansell, S. M. Functionalised N-Heterocyclic Carbene Ligands in Bimetallic Architectures. *Chem. Eur. J.* **2020**, *26*, 5927–5941.

(4) Huynh, H. V. *The Organometallic Chemistry of N-Heterocyclic Carbenes*; John Wiley & Sons, Ltd, **2017**.

(5) Hoshimoto, Y.; Kinoshita, T.; Ohashi, M.; Ogoshi, S. A Strategy to Control the Reactivation of Frustrated Lewis Pairs from Shelf-Stable Carbene Borane Complexes. *Angew. Chem. Int. Ed.* **2015**, *54*, 11666–11671.

(6) Hoshimoto, Y.; Asada, T.; Hazra, S.; Kinoshita, T.; Sombut, P.; Kumar, R.; Ohashi, M.; Ogoshi, S. Strategic Utilization of Multifunctional Carbene for Direct Synthesis of Carboxylic–Phosphinic Mixed Anhydride from CO2. *Angew. Chem. Int. Ed.* **2016**, *55*, 16075–16079.

(7) Asada, T.; Hoshimoto, Y.; Ogoshi, S. Rotation-Triggered Transmetalation on a Heterobimetallic Cu/Al N-Phosphine-Oxide-Substituted Imidazolylidene Complex. *J. Am. Chem. Soc.* **2020**, *142*, 9772–9784.

(8) Yamauchi, Y.; Hoshimoto, Y.; Kawakita, T.; Kinoshita, T.; Uetake, Y.; Sakurai, H.; Ogoshi, S. Room-Temperature Reversible Chemisorption of Carbon Monoxide on Nickel(0) Complexes. *J. Am. Chem. Soc.* **2022**, *144*, 8818−8826.

(9) Yamauchi, Y.; Mondori, Y.; Uetake, Y.; Takeichi, Y.; Kawakita, T.; Sakurai, H.; Ogoshi, S.; Hoshimoto, Y. Reversible Modulation of the Electronic and Spatial Environment around Ni(0) Centers Bearing Multifunctional Carbene Ligands with Triarylaluminum. *J. Am. Chem. Soc.* **2023**, *145*, 16938–16947.

(10) Branzi, L.; Franco, D.; Baron, M.; Armelao, L.; Rancan,

M.; Sgarbossa, P.; Biffis, A. Palladium(II) Complexes with N-Phosphine Oxide-Substituted Imidazolylidenes (PoxIms): Coordination Chemistry and Catalysis. *Organometallics* **2019**, *38*, 2298–2306.

(11) Branzi, L.; Baron, M.; Armelao, L.; Rancan, M.; Sgarbossa, P.; Graiff, C.; Pöthig, A.; Biffis, A. Coordination Chemistry of Gold with: N-Phosphine Oxide-Substituted Imidazolylidenes (POxIms). *New J. Chem.* **2019**, *43*, 17275–17283.

(12) Hoshimoto, Y.; Ogoshi, S. Development of Metal Complexes Equipped with Structurally Flexible Carbenes. *Bull. Chem. Soc. Jpn.* **2021**, *94*, 327–338.

(13) Tolman, C. A. Electron Donor-Acceptor Properties of Phosphorus Ligands. Substituent Additivity. *J. Am. Chem. Soc.* **1970**, *92*, 2953–2956.

(14) Huynh, H. V.; Han, Y.; Jothibasu, R.; Yang, J. A. ^{13}C NMR Spectroscopic Determination of Ligand Donor Strengths Using N-Heterocyclic Carbene Complexes of Palladium(II). *Organometallics* **2009**, *28*, 5395–5404.

(15) Teng, Q.; Huynh, H. V. A Unified Ligand Electronic Parameter Based On13C NMR Spectroscopy of N-Heterocyclic Carbene Complexes. *Dalton Trans.* **2017**, *46*, 614–627.

(16) Liske, A.; Verlinden, K.; Buhl, H.; Schaper, K.; Ganter, C. Determining the π-Acceptor Properties of n-Heterocyclic Carbenes by Measuring the 77Se NMR Chemical Shifts of Their Selenium Adducts. *Organometallics* **2013**, *32*, 5269–5272.

(17) Dorta, R.; Scott, N. M.; Costabile, C.; Cavallo, L.; Hoff, C. D.; Nolan, S. P. Steric and Electronic Properties of N-Heterocyclic Carbenes (NHC): A Detailed Study on Their Interaction with Ni(CO)4. *J. Am. Chem. Soc.* **2005**, *127*, 2485–2495.

(18) If standard deviation is to be ignored in the Tolman electronic parameter, the unsaturated analogues **2b** and **2c** would have a rather unexpected stronger net donicity compared to their saturated counterparts, and the (S)PoxIms would be marginally stronger donors than the classical (S)IPr and (S)IMes.

(19) Hansch, C.; Leo, A.; Taft, R. W. A Survey of Hammett Substituent Constants and Resonance and Field Parameters. *Chem. Rev.* **1991**, *91*, 165–195.

(20) Huynh, H. V.; Han, Y.; Ho, J. H. H.; Tan, G. K. Palladium(II) Complexes of a Sterically Bulky, Benzannulated N-Heterocyclic Carbene with Unusual Intramolecular C-H···Pd and $C_{carbene}$···Br Interactions and Their Catalytic Activities. *Organometallics* **2006**, *25*, 3267–3274.

(21) Denk, M. K.; Rodezno, J. M.; Gupta, S.; Lough, A. J. Synthesis and Reactivity of Subvalent Compounds: Part 11. Oxidation, Hydrogenation and Hydrolysis of Stable Diamino Carbenes. *J. Organomet. Chem.* **2001**, *617–618*, 242–253.

(22) van Lierop, B. J.; Reckling, A. M.; Lummiss, J. A. M.; Fogg, D. E. Clean, Convenient, High-Yield Access to Second-Generation Ru Metathesis Catalysts from Commercially Available Precursors. *ChemCatChem* **2012**, *4*, 2020–2025.

(23) Günay, M. E.; Özdemir, N.; Ulusoy, M.; Uçak, M.; Dinçer, M.; Çetinkaya, B. The Influence of Moisture on Deprotonation Mode of Imidazolinium Chlorides with Palladacycle Acetate Dimer. *J. Organomet. Chem.* **2009**, *694*, 2179–2184.

(24) Wu, W.; Teng, Q.; Chua, Y. Y.; Huynh, H. V.; Duong, H. A. Iron-Catalyzed Cross-Coupling Reactions of Arylmagnesium Reagents with Aryl Chlorides and Tosylates: Influence of Ligand Structural Parameters and Identification of a General N-Heterocyclic Carbene Ligand. *Organometallics* **2017**, *36*, 2293–2297.

(25) Yang, L.; Powell, D. R.; Houser, R. P. Structural Variation in Copper(i) Complexes with Pyridylmethylamide Ligands: Structural Analysis with a New Four-Coordinate Geometry Index, T4. *J. Chem. Soc., Dalton Trans.* **2007**, No. 9, 955–964.

(26) Tao, W.; Akita, S.; Nakano, R.; Ito, S.; Hoshimoto, Y.; Ogoshi, S.; Nozaki, K. Copolymerisation of Ethylene with Polar Monomers by Using Palladium Catalysts Bearing an N-Heterocyclic Carbene-Phosphine Oxide Bidentate Ligand. *Chem. Commun.* **2017**, *53*, 2630–2633.

(27) Huynh, H. V.; Wong, L. R.; Ng, P. S. Anagostic Interactions and Catalytic Activities of Sterically Bulky Benzannulated N-Heterocyclic Carbene Complexes of Nickel(II). *Organometallics* **2008**, *27*, 2231–2237.

(28) Gu, Y.; Kar, T.; Scheiner, S. Fundamental Properties of the CH ··· O Interaction: Is It a True Hydrogen Bond? *J. Am. Chem. Soc.* **1999**, *121*, 9411–9422.

(29) Scheiner, S.; Gu, Y.; Kar, T. Evaluation of the H-Bonding Properties of CH···O Interactions Based upon NMR Spectra. *J. Mol. Struct. Theochem.* **2000**, *500*, 441–452.

(30) Steiner, T. Unrolling the Hydrogen Bond Properties of C-H···O Interactions. *Chem. Commun.* **1997**, 727–734.

(31) Steiner, T.; Desiraju, G. R. Distinction between the Weak Hydrogen Bond and the van Der Waals Interaction. *Chem. Commun.* **1998**, 891–892.

(32) Huynh, H. V. Electronic Properties of N-Heterocyclic Carbenes and Their Experimental Determination. *Chem. Rev.* **2018**, *118*, 9457−9492.

(33) Nguyen, V. H.; El Ali, B. M.; Huynh, H. V. Stereoelectronic Flexibility of Ammonium-Functionalized Triazole-Derived Carbenes: Palladation and Catalytic Activities in Water. *Organometallics* **2018**, *37*, 2358–2367.

(34) Clark, D. T.; Murrell, J. N.; Tedder, J. M. The Magnitudes and Signs of the Inductive and Mesomeric Effects of the Halogens. *J. Chem. Soc.* **1963**, 1250–1253.

(35) Murrell, J. N. The Electronic Spectrum of Aromatic Molecules VI: The Mesomeric Effect. *Proc. Phys. Soc. Sect. A* **1955**, *68*, 969–975.

(36) Kerber, R. C. If It's Resonance, What Is Resonating? *J. Chem. Educ.* **2006**, *83*, 223–227.

(37) Nguyen, V. H.; Dang, T. T.; Nguyen, H. H.; Huynh, H. V. Platinum(II) 1,2,4-Triazolin-5-Ylidene Complexes: Stereoelectronic Influences on Their Catalytic Activity in Hydroelementation Reactions. *Organometallics* **2020**, *39*, 2309–2319.

(38) Teng, Q.; Huynh, H. V. Determining the Electron-Donating Properties of Bidentate Ligands by ^{13}C NMR Spectroscopy. *Inorg. Chem.* **2014**, *53*, 10964–10973.

(39) Lo, W. K. C.; Huff, G. S.; Cubanski, J. R.; Kennedy, A. D. W.; McAdam, C. J.; McMorran, D. A.; Gordon, K. C.; Crowley, J. D. Comparison of Inverse and Regular 2-Pyridyl-1,2,3-Triazole "Click" Complexes: Structures, Stability, Electrochemical, and Photophysical Properties. *Inorg. Chem.* **2015**, *54*, 1572–1587.

(40) Leung, J. N.; Luong, H. T. T.; Huynh, H. V. Stereoelectronic Profiling of Neutral and Monoanionic Biimidazoles and Mixed Diimines. *Inorg. Chem.* **2023**, *62*, 4606–4617.

(41) Diaz-Rodriguez, R. M.; Robertson, K. N.; Thompson, A. Classifying Donor Strengths of Dipyrrinato/Aza-Dipyrrinato Ligands. *Dalton Trans.* **2019**, *48*, 7546–7550.

(42) Leung, J. N.; Huynh, H. V. Stereoelectronic Mapping of Dithiocarbamates and Xanthates. *Inorg. Chem.* **2023**, *62*, 295–303.

(43) Do, D. C. H.; Huynh, H. V. Controlled Access to Four- and Six-Membered Palladacycles via Modifying Donor Abilities of β-Ketiminato Ligands ("NacAcs"). *Inorg. Chem.* **2022**.
(44) Yan, X.; Feng, R.; Yan, C.; Lei, P.; Guo, S.; Huynh, H. V. A Palladacyclic N-Heterocyclic Carbene System Used to Probe the Donating Abilities of Monoanionic Chelators. *Dalton Trans.* **2018**, *47*, 7830–7838.
(45) Verlinden, K.; Buhl, H.; Frank, W.; Ganter, C. Determining the Ligand Properties of N-Heterocyclic Carbenes from 77Se NMR Parameters. *Eur. J. Inorg. Chem.* **2015**, 2416–2425.
(46) Nelson, D. J.; Nahra, F.; Patrick, S. R.; Cordes, D. B.; Slawin, A. M. Z.; Nolan, S. P. Exploring the Coordination of Cyclic Selenoureas to Gold(I). *Organometallics* **2014**, *33*, 3640–3645.

The electronic properties of *N*-phosphine oxide functionalized imidazoli(di)n-2-ylidenes have been examined by experimental methods, and they are found to be slightly weaker σ-donors but stronger π-acceptors compared to the analogous common NHCs.

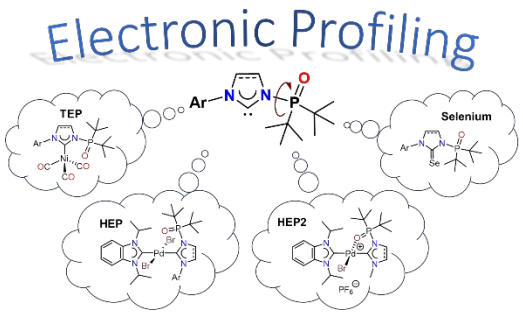

For Table of Contents Only